Chapter 10

Reused Lithium-Ion Battery Applied in Water Treatment Plants

Yi-Hsien Chiang and Wu-Yang Sean

Additional information is available at the end of the chapter

http://dx.doi.org/10.5772/intechopen.76303

Abstract

For stabilizing renewable energies and shaving peak power at noon, both the energy consumption and potential renewable energies in Dihua waste water treatment plant (WWTP) in Taiwan are analyzed. Under the consideration of environment, cost, and performance, automotive reused lithium-ion battery (RLIB) is employed. Two typical automotive lithium-ion batteries are used in this study after the selection of suitable battery cells. In particular, one simple, converterless energy management system (EMS) is developed and integrated in new RLIB packs. The control strategy between RLIB and an additional physical battery is adjusted by simulation. An online estimation of RLIB's internal resistance and open-circuit voltage monitoring scheme is applied in EMS to ensure the safety of RLIB. The bench test and rough economical estimation reveal that EMS shows great potential in elongating life cycle and possibly benefits from feed-in tariff and peak shift of electricity charges.

Keywords: reused lithium-ion battery (RLIB), wastewater treatment plant (WWTP), energy management system (EMS), peak shift, feed-in tariff (FIT)

1. Introduction

The Dihua wastewater treatment plant (WWTP) is between the Tamsui and Keelung Rivers in Taipei. It treats sewage from Taipei City's household connections and interception stations. The plant, which has a capacity of 500,000 m^3/day, is the largest secondary treatment plant in Taiwan. Water Resources Agency (WRA) in Taiwan recently launched several projects to promote energy self-efficient WWTPs. Their action plan is to employ green energy sources in WWTP by collocating with efficient new water treatment processes. Green energy sources refer to well-known renewable energy sources (e.g., biomass, wind energy, solar energy, hydropower, and local waste heat).

Some projects in the world originated from the concept of the energy–water nexus, which is the coupling of energy, water, the environment including climate change, and food supply [1–9]. Studies conducted on WWTP and in collaboration with local governments and major organizations provide solid evidence of unit electricity for wastewater treatment or neutral energy. Electricity from renewable energy resources, such as wind or solar power, may be used to partially or completely replace electricity from the grid. Moreover, novel wastewater treatment processes have been employed in WWTPs to reduce the energy requirements per unit volume of treated wastewater in comparison with cases that depend on electricity only from renewable energy resources [10–15]. Some researchers illustrated that energy cannot be gained at all from aerobic digestion or organic substances at WWTPs and sludge treatment plants. The specific energy demand at these plants is still high, and too much energy is needed for far-reaching aerobic degradation of organic substances. However, biogas from anaerobic treatment from WWTPs or waste management may become a suitable way of improving energy efficiency. For alternative sanitation concepts, sewage and food waste management, or other environmental assessments of urban water systems [16, 17], life cycle assessments should be conducted to explore plant energy balance. Besides renewable energy, one potential candidate for compensating the consumption at WWTPs is wastewater heat recovery. Case studies show that technologies for heat recovery from wastewater also have been successfully implemented. However, heat recovery may harm the wastewater treatment process and reduce the performance of WWTPs [18–26].

Lithium-ion batteries contain precious metals such as lithium, cobalt, or manganese; therefore, recycling and recuperation of these batteries are highly advantageous. However, these processes use high levels of electricity in traditionally chemical methods [27–32]. Lithium-ion batteries are suitable as ancillary services or for supporting large-scale solar and wind integration in existing power systems by providing grid stabilization or frequency regulation [50]. Lithium-ion batteries are also classified as dangerous waste. If they are not properly treated, then they will damage the environment and cause harm to humans and the environment. By contrast, abundant electrical capacity remains in discarded lithium-ion batteries. Following an intensive review on advanced smart metering and communication infrastructures, a strategy for integrating electric vehicles (EVs) into the electric grid is presented [51]. Under the vehicle-to-grid phenomenon, the deployment of EV batteries in the energy market can compensate for fluctuations of the electric grid. A previous study [52] presented the optimization of electrical energy storage systems and improved control strategies based on hybrid power source and series.

To achieve energy self-efficient WWTPs, we consider several ways of ensuring positive energy balance of wastewater treatment such as renewable energies. In this study, automotive reused lithium-ion battery (RLIB) is used to accumulate electricity at night to shave peak power in the grid at noon as a prior phase before chemical separation of the RLIB pack. In general, RLIB packs might decay rapidly after being discarded, and the energy management system (EMS) is developed to address this issue. The performance of depth of discharge (DoD), which indicates the life cycle, is used to determine the effectiveness of EMS in bench test. Besides, an online scheme of estimating life cycle sensitized parameters is embedded in EMS for safety and performance guarantee.

http://dx.doi.org/10.5772/intechopen.76303

2. Analysis of energy consumption and potential renewable energies

After dividing a portion of effluent from the Dihua Sewage Pumping Station in Taipei, sewage enters the Dihua WWTP at an average of 434,349 m^3/day. It then passes through fine bar screens to remove coarse materials. It flows into primary clarifiers to remove the greater part of the suspended solids and a small portion of the organic matter in the sewage. Aeration basins and secondary clarifiers are used to remove organic matter in the sewage. The effluent from the secondary clarifiers is disinfected with sodium hypochlorite to remove pathogens before discharge into the Tamsui River. After sand filtration, 10,000 cubic meters per day of effluent become reused water for the plant. Night solids, combined with primary sludge and secondary sludge, is thickened, anaerobically digested, and dewatered to become sludge cake. It is then disposed in a landfill site or used as fertilizer for inedible vegetation by any organization that requests it. The energy consumption is listed in **Table 1**.

In the Dihua plant, the entire water treatment process consumes 120,526 kWh of electricity a day. Approximately 0.28kWh/m^3 is required for wastewater treatment. This value is much lower than UNESCO's report (2014) of 0.62–0.87 kWh/m^3 excluding pumping to the treatment site and equipment efficiency. The average quantity of energy used varies considerably depending on the level of treatment, type of treatment, and size of plant, but it approximately doubles from primary to secondary and doubles again to tertiary levels of treatment (US EPA Office of Water 2013).

In Dihua's case, the outcome of biomass occupies 55.69% total unstable renewable energy as listed in **Figures 1** and **2**. Twenty percent of total area is assumed to be installed solar panel, and the reliable electricity capacity of 943.8 kW is obtained. Hydropower and wind power are not dominant energy resources in this plant.

Process	(%)	Energy consumption (kWh/day)	Energy demand unit volume (kWh/m^3)
Aerobic digestion	25.47	30697.67	0.0706
Sludge treatment	6.15	7416.02	—
Secondary clarifier	5.40	6503.03	0.0149
Wastewater pumping	5.12	6167.67	—
Solid dewatering	3.28	3954.15	—
Lighting and building	3.22	3875.41	—
Disinfection	2.28	2750.31	0.0063
Grit	0.67	807.31	0.0018
Primary clarifier	0.47	571.32	0.0013
Anaerobic digester	1.09	1318.28	—
Aeration	46.85	56465.37	0.13
Total	100	120526.57	—

Table 1. Usage of energy consumption in Dihua WWTP.

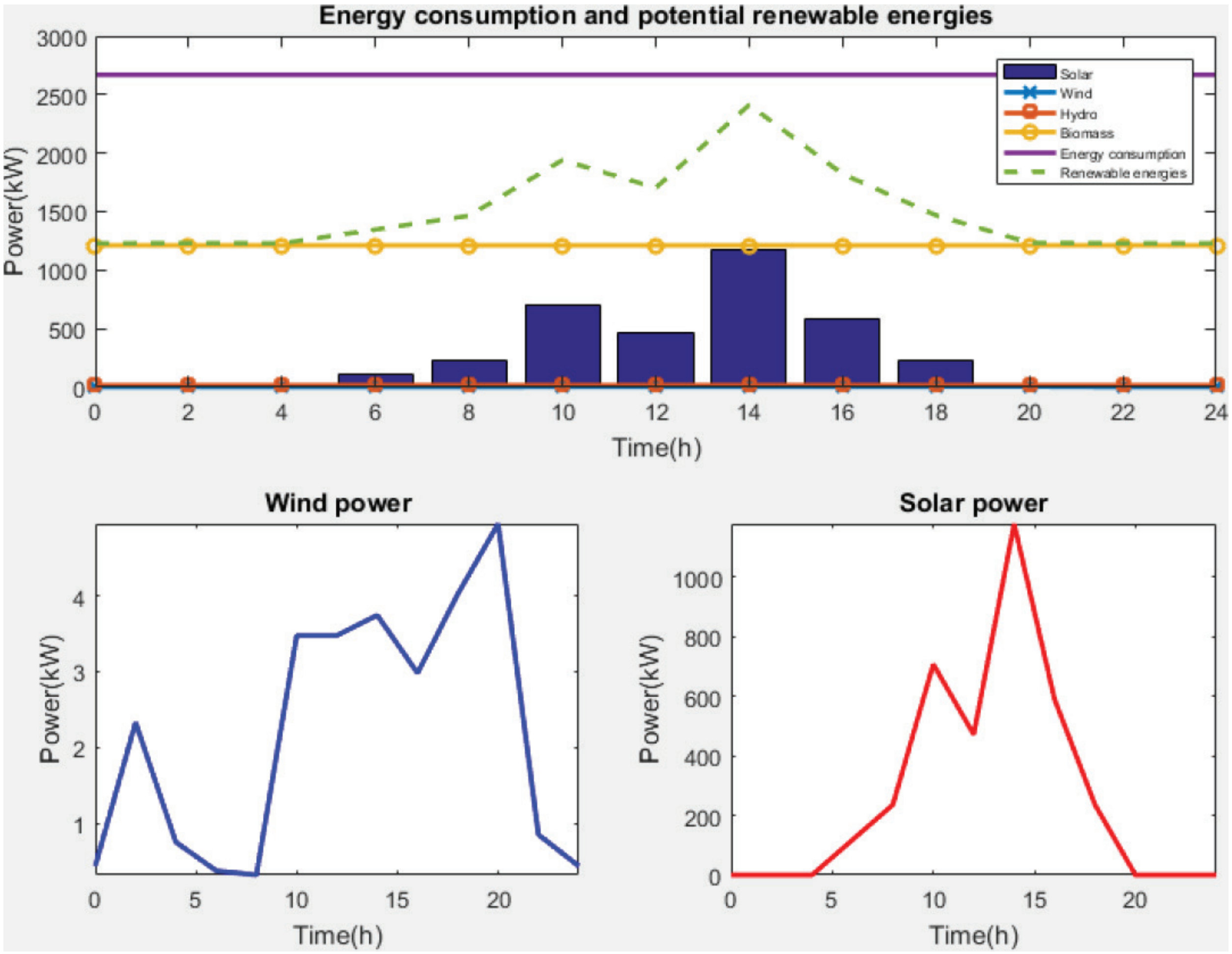

Figure 1. Unsteady renewable energies in Dihua WWTP.

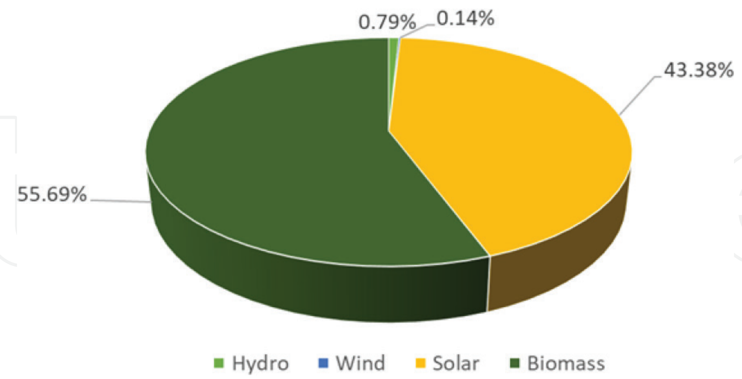

Figure 2. Potential renewable energies in Dihua WWTP.

3. Motivation of using RLIB

Demand for urban vehicles focusing on sustainable transportation has prompted a substantial trend towards automotive electrification such as hybrids and EVs. With more than 70% of EVs likely to be introduced in 2015 with Li-ion based battery chemistry, the recycling of Li-ion has

http://dx.doi.org/10.5772/intechopen.76303

Figure 3. Reused Lithium-ion battery used in pure electric vehicles (left: $LiFePO_4$, right: $LiMnNiCoO_2$).

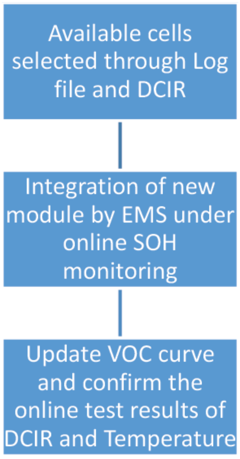

Figure 4. Flowchart of RLIB.

Figure 5. About 8 hectares huge space in the second deck of aeration tank in Dihua plant.

become a crucial topic in the automotive industry. When the battery packs in a lithium-ion-powered vehicle are deemed too worn out for driving, they still have up to 80% of their capacity left. Before they ever arrive in a recycling center, these batteries are used to prop up the grid, especially alongside energy sources that may not be quite as steady, such as wind or solar power

(**Figure 2**). Furthermore, the cost of RLIB is roughly cheaper than 1/3 of a new battery. This merit enhances strong competition compared with other cheap flow batteries or NAS batteries.

For instance, two packs of RLIBs are shown in **Figure 3**. Both of them are originally applied in pure EVs. After working for several years, they are used as experimental targets before cycling and recuperation by chemical method. In this study, two different types of packs are selected. The flowchart in **Figure 4** shows that suitable cells are activated and selected based on log file and DC internal resistance, and each new module is assembled with EMS. Subsequently, the module is installed in a test bench to update voltage of open circuit (VOC). In addition to establishing water, energy, and reusing nexus in urban areas, the Dihua WWTP is chosen for its large area of 8 hectares. Thus, an extensive enclosed space is available for placing RLIB between the aeration tank and green park in the ground (**Figure 5**).

4. Benefit of energy management in WWTP

Reducing variability in renewable energy is crucial in managing the peaks in WWTP. As a result, this strategy is dispensable for employing energy storage systems charging during off peak times and injecting energy into smart grids during peak times. Benefits can be estimated from the low price at night, cost of basic contract fee of electricity, and effect of frequency regulation.

Results of the economic benefit assessment are shown in **Table 2**. We assume that renewable energy's purchase price is 0.143 USD. Renewable energy is assumed to be fully fed back to the grid. About 80% of the total RLIB is used as night storage, and the cost of RLIB is 133USD unit kWh. In the case of Dihua plant, the calculation of RLIB demand is 32,106 kWh, which is roughly equivalent to 3200 pure EV battery pack. This value is also about 1/20 of the total number of domestic sales of EVs from 2011 to 2016 in Taiwan. The initial cost of RLIB packs is 4.3 million USD. However, only the sales of renewable energy power into the grid based on feed-in tariff (FIT) are 1.68 million USD. The annual electricity rate difference at noon and night is 140.6 million NTD, and the annual income at noon and night is 4.69 million USD. Therefore, the plant can break even in 2 years and continue to profit each year without considering the installation fee. Other plants also show similar profitable results such as Dihua plant in **Table 2**.

<table>
<tr><td colspan="4" rowspan="3">Assumption:
1. Feed-in tariff is averaged approximated as NTD$4.3 without considering the resources.
2. Renewable energies are totally feeback into grid, and averaged use rate of RLIB is 80%.
3. In this study, the set up expense of RLIB is not considered.</td><td>Cost of RLIB(NTD$/kWh)</td><td>4000</td><td>Peak time(o'clock)</td><td>7~22</td></tr>
<tr><td>Benefit of feed-in biomass(NTD$)</td><td>3.92</td><td>Price gap at peak and off peak(NTD$)</td><td>1.5</td></tr>
<tr><td>Benefit of feed-in solar(NTD$)</td><td>4.67</td><td>Averaged use rate of RLIB</td><td>0.8</td></tr>
<tr><td>Plant name</td><td>Anuual energy consumption (kWh)</td><td>Potential renewable energies(kWh)</td><td>Utilization rate of renewable energies(%)</td><td>Capacity of battery required(kWh)</td><td>Battery cost(NTD$*10^{-4})</td><td>Feed-in benefit(NTD$*10-4)</td><td>Benefit of shaving power(NTD$*10-4)</td></tr>
<tr><td>Dihua</td><td>23382265</td><td>11718800</td><td>50%</td><td>32106</td><td>$12,843</td><td>$5,039</td><td>$1,406</td></tr>
<tr><td>Taoyuan</td><td>2630349</td><td>1863911</td><td>71%</td><td>5107</td><td>$2,043</td><td>$801</td><td>$224</td></tr>
<tr><td>Taichung</td><td>6095701</td><td>1696606</td><td>28%</td><td>4648</td><td>$1,859</td><td>$730</td><td>$204</td></tr>
<tr><td>Hsinchu</td><td>2177068</td><td>2822642</td><td>130%</td><td>7733</td><td>$3,093</td><td>$1,214</td><td>$339</td></tr>
<tr><td>Tainan</td><td>8512309</td><td>3269845</td><td>38%</td><td>8958</td><td>$3,583</td><td>$1,406</td><td>$392</td></tr>
</table>

Table 2. Benefit assessment of 5 WWTPs applying RLIB (NTD; 30NTD = 1USD).

5. Development of EMS

To reduce the peak current in LIB pack, a physical battery is employed in LIB effectively, but range extension is still limited in the case study [33]. The effect of life cycle extension is discussed [34] by the transient supply of physical battery. Given the traditional large DC/DC converter in EMS, a small prototype of DC-DC and simple circuit may be proposed to isolate the battery pack and not harvest energy from random peak power [35, 36]. The scenarios of usage cover the regenerative power supply and charging/discharging between individual and physical batteries. Some studies have focused on the design of levering DC-DC converter [37, 38], but several researchers have introduced a converterless circuit in EVs based on a DC inverter [39, 40]. The literature implies the possibility of EMS with high efficiency and low cost. Specific control strategies including neutral networks are illustrated in [40–42]. Economic analysis shows that the high price of LIB leads to superior benefits in elongating life cycle. Real-time simulators are a powerful platform before on-board tests [42]. In [43], a simple circuit of elongating life cycle life was reported. Without a complex DC-DC converter, only duty control using a suitable physical battery can narrow DoD of LIB and elongate the life cycle of batteries [44–48]. **Figure 6** shows the relationship between DoD and life cycle. None of the lines in **Figure 8** are linear, thereby indicating that DoD plays a major role in gaining life cycle.

Figure 7 shows a simple, converterless parallel circuit. EMS can achieve active control by switching the discharging ratio between LIB and auxiliary physical battery at unit time. The architecture of EMS is shown in **Figure 8**. It is modified from battery management system. EMS is disposed as an interface among RLIB, auxiliary physical battery (ultracapacitor, UC), and systematic grid. The control strategy aims to keep the switch periodically close and open by a predetermined duty cycle, namely, the sharing ratio of RLIB's loading controlled by EMS. In detail, EMS generates a PWM (pulse width modulation) signal to control the on/off time of the lower arm of the switch module.

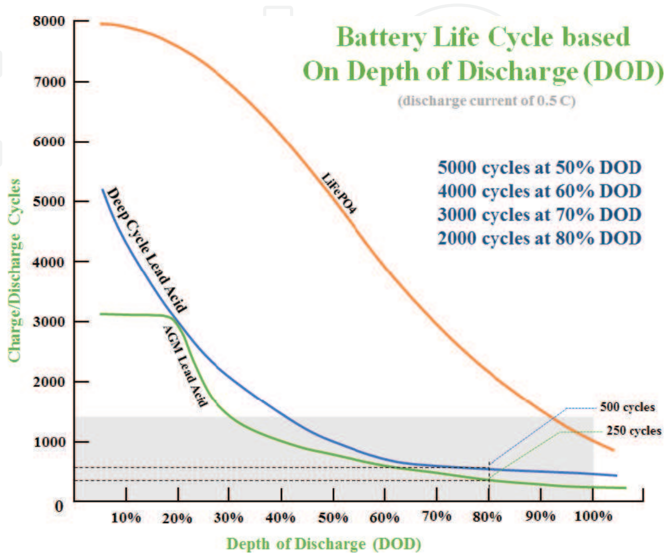

Figure 6. Relationship between DoD and charge/discharge cycles (life cycles) modified from [49].

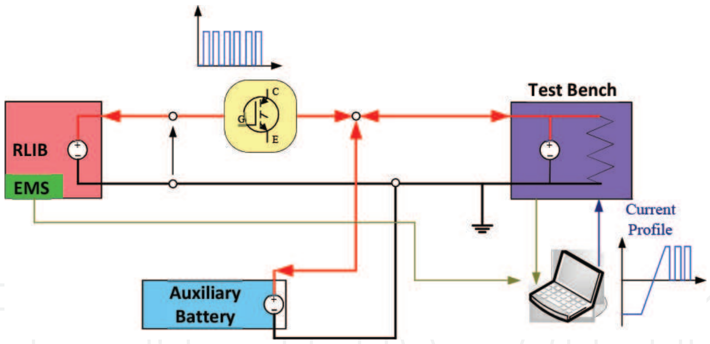

Figure 7. RLIB in parallel connection with auxiliary physical battery (ultracapacitor) controlled by EMS.

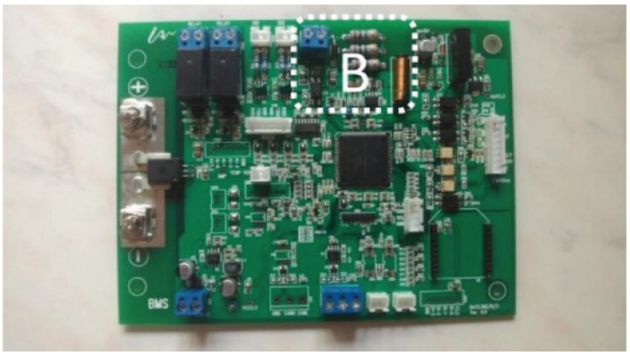

Figure 8. Architecture of EMS (symbol B is a safety device for estimating RLIB pack's insulation resistance).

6. Real-time simulator for optimizing the sharing ratio between RLIB and UC

Real-time simulators have been widely used in developing and verifying control strategies for power systems. Such devices are a powerful platform before on-board tests. Total analytical modules including EMS module is employed in the simulator. Detailed topology can be found in [41, 42]. In the system level, the control strategy from the vehicle side for the powertrain relating to the area electric range is validated [15]. Through the vehicle side, commands of torque and speed are sent out to the demand side of the motor simultaneously. Likewise, commands for gear shifting commands, the auxiliary system, and protection signals are passed from the vehicle side to other control units. It is originally developed in the environment of OPAL-RT®. An imaginary vehicle module is linked with the simulator via an analog/digital I/O interface, CAN bus, and RS-232. The off-line environment connected to real-time simulator provides sufficient capability for the development of EMS to select the optimized current sharing ratio between LIB and UC. The environment and interface model the dynamic response of load, multi-battery pack, and EMS.

7. Monitoring state of health (SOH)

State of charge and SOH define the most important amounts of charge and rated capacity loss of a battery, respectively. To determine these two parameters instantaneously, VOC

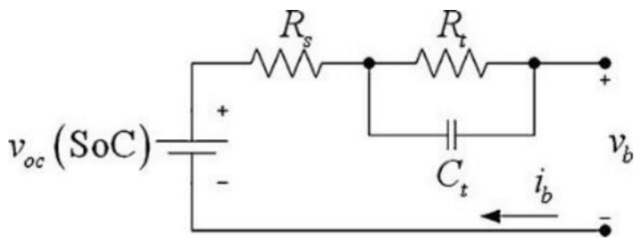

Figure 9. A generalized ECM for lithium batteries.

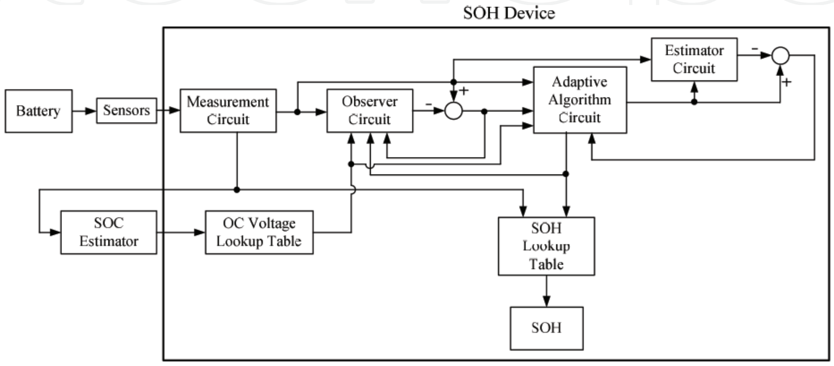

Figure 10. A flowchart describes how SoH functions.

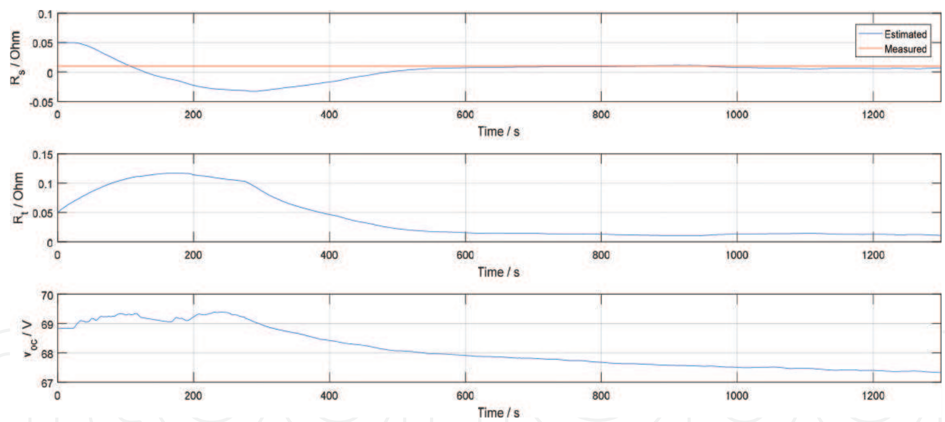

Figure 11. Comparison of estimated and measured internal resistances (1st, R_s; 2nd, R_t) and VoC (voltage of open circuit) in test case.

and internal resistance (IR) of the battery are indispensable. To guarantee the safety of RLIB, besides the insulation monitoring function shown in **Figure 8**, a simple, training-free, and easily implemented scheme in EMS is applied. This scheme is capable of estimating VOC and IR, particularly here for RLIB pack [53]. On the basis of an equivalent circuit model (ECM) shown in **Figure 9**, the electrical performance of the battery can be formulated into state-space representation. An underdetermined model's parameters can be arranged linearly so that an adaptive control approach can be applied. An algorithm of adaptive control is developed by exploiting the Lyapunov stability criteria as briefly illustrated in **Figure 10**. VOC and IR can be extracted precisely without limitations of input signals in the system, such as persistent excitation (PE). It enhances the application of this method for power systems. **Figure 11** shows one example for examining the algorithm by using adaptive control observer to estimate VOC and IR through the adaptive control approach. Estimation of SOH-sensitized IR can converge into a stable measured value in about 600(s).

8. Bench-test set-up and procedure

Two packs of RLIB are shown in **Figure 3**. Both of them are originally applied in pure EVs. After running on board for several years, they are used as experimental targets in this study, assembled with EMS, and installed in a test bench to simulate RLIB at WWTP.

Two types of LIB cells with a large difference in IR are employed in this study, and the specifications are listed in **Table 3**. An automated test bench with rated voltage and current of 500 V/450 A is utilized for the test. The initial rated voltage of RLIB is 70 V. A power pattern converted from the daily usage of electricity in WWTP is programmed into the machine for discharge/charge operation. In this study, all components are integrated in the laboratory, and the pattern of electricity is chosen for simulating the intermittent charging/discharging cycle of renewable energy and power accumulation due to the lack of in-situ energy consumption data. The duty cycle, current, and voltage of the RLIB terminal are monitored by the EMS. A total of 21 cells of LiFePO4 RLIB and three modules of LiMnNiCoO2 RLIB are modularized into two individual packs. A test case of RLIB connected with EMS is shown in **Figure 12**.

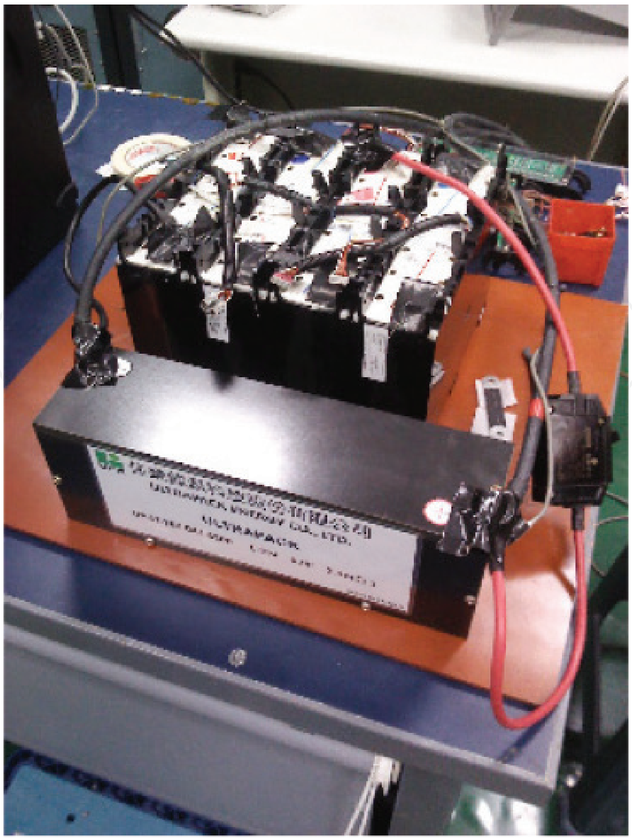

Figure 12. Implementation of RLIB with EMS and auxiliary physical battery (left: EMU; Central: $LiFePO_4$ LIB pack; and right: auxiliary physical battery).

Item	Unit	Energy density (Wh/kg)	IR(mΩ)	
			Pack	Total*
Molicel Module 10.96 V EME335-I403 (18650AG, 3S35P)	3 modules	100	3.27 × 3	
Pishuang Cell 38.4 Ah 3.2 V 400013201	21 cells	60	65.75	84.23

*Total IR is composed of internal resistance + harness resistance + fixture resistance.

Table 3. Specification of RLIB.

9. Verification of RLIB pack with EMS

To consider a real severe case, the current draw of the pattern of electricity is imposed on the RLIB pack [41, 42]. As shown in **Figure 13**, the accuracy of simulation with RLIB analytical module is examined by comparing with the measured results. The simulation with assumed linear VOC yields the deviation from the measured voltage curve. Otherwise, the simulation accurately predicts the response of RLIB.

Simulation results regarding voltage drop of a single RLIB pack in 100(s) under random load current is compared with the other case of RLIB pack connected with UC and active controlled by EMS (**Figures 14** and **15**). Effect of active controlled by EMS represented in DoD is not obvious. However, the energy consumption estimated from I^2*IR at both cases is shown in **Figures 16** and **17**, and EMS decreases 26% heat loss of RLIB.

In the bench test, the first case of $LiMnNiCoO_2$ RLIB pack in **Figure 18** shows the comparison of DoD with/without EMS under constant c-rate discharging. RLIB in active control of duty cycle 60% (solid line) shows the more stable and limit DoD than a single RLIB pack (dash line). Through real-time simulation by monitoring DoD, we optimize the best control duty of 60%. Here, IR of the RLIB pack plays an essential role in the distribution of DoD. To examine the control strategy even further, LiFePO4 RLIB is utilized as the DoD results (**Figure 19**). The effectiveness of EMS (solid line) is realized in comparison with the cases without EMS (point line) and single $LiFePO_4$ RLIB (dash line). To consider the stable DoD distribution of RLIB by using

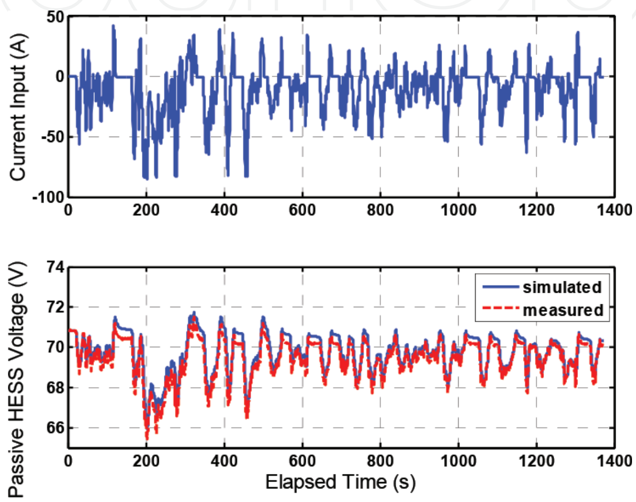

Figure 13. Comparison of simulation and measured results (upper: current; down: voltage) [41].

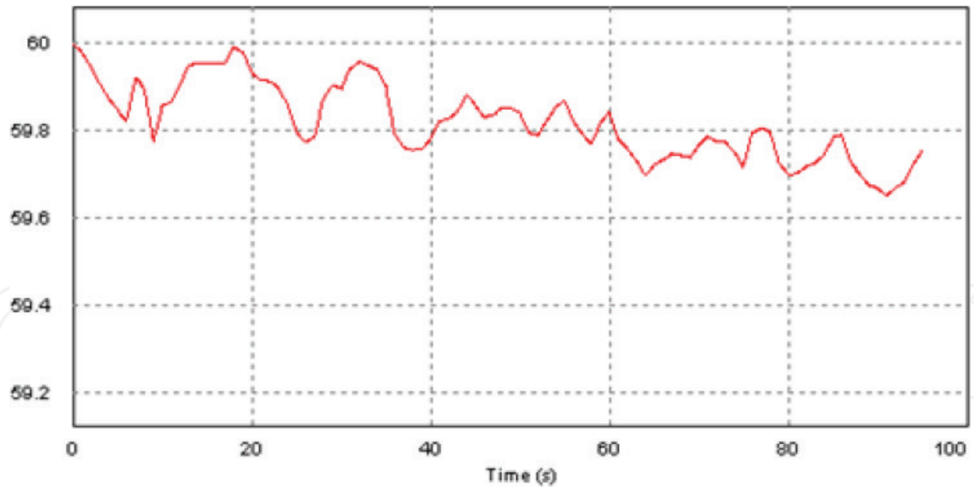

Figure 14. Voltage drop in simulation of 60 V single RLIB pack.

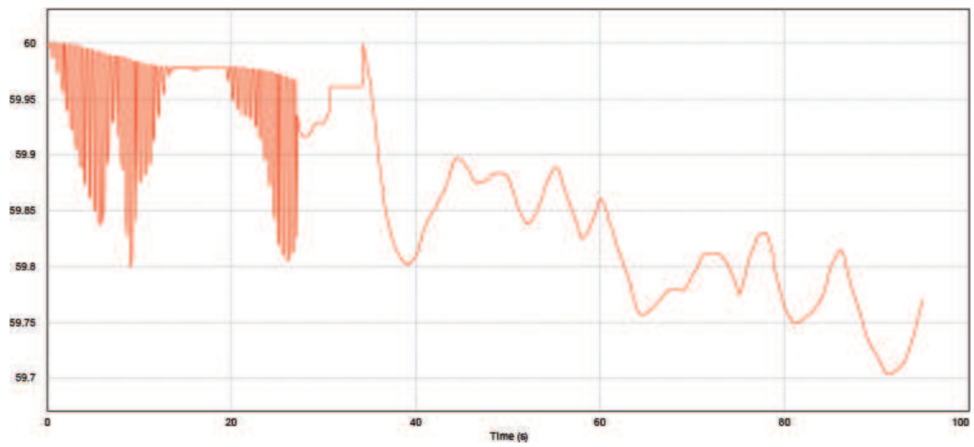

Figure 15. Voltage drop of 60 V RLIB pack which is in parallel connect with UC and active controlled by EMS.

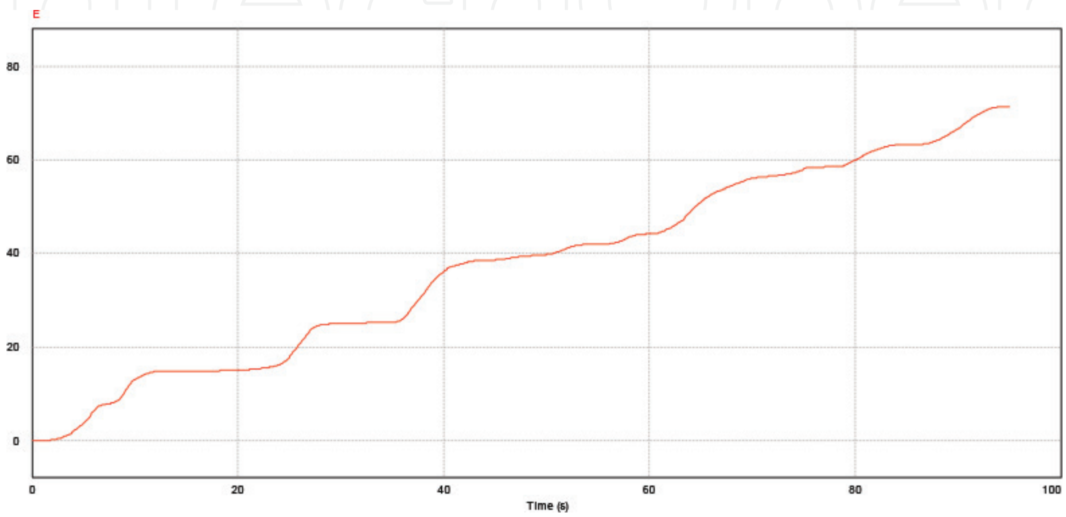

Figure 16. The energy consumption in the case of **Figure 14** (70 J) calculated by simulation.

http://dx.doi.org/10.5772/intechopen.76303

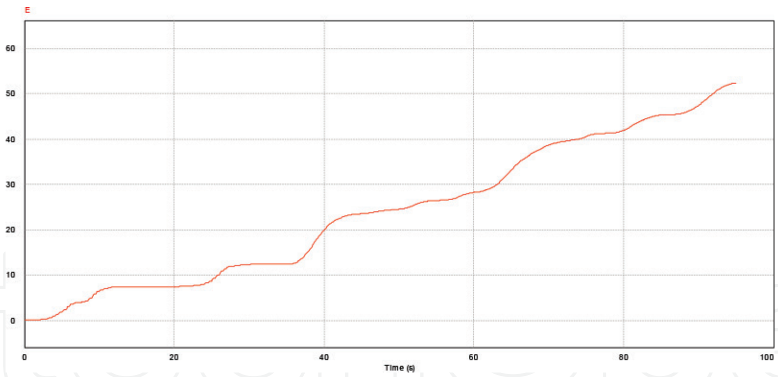

Figure 17. The energy consumption in the case of **Figure 15** (52 J).

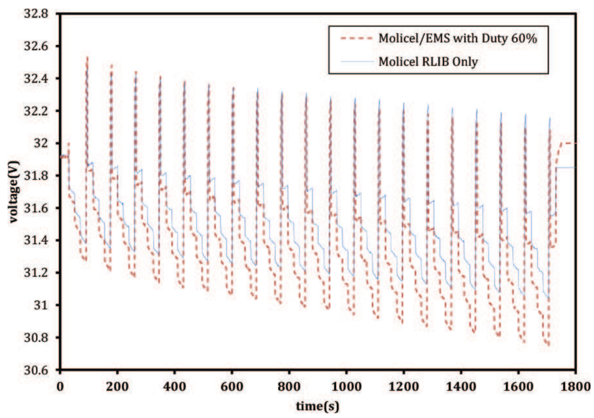

Figure 18. Comparison of DoD in single $LiMnNiCoO_2$ RLIB pack and RLIB with/without control.

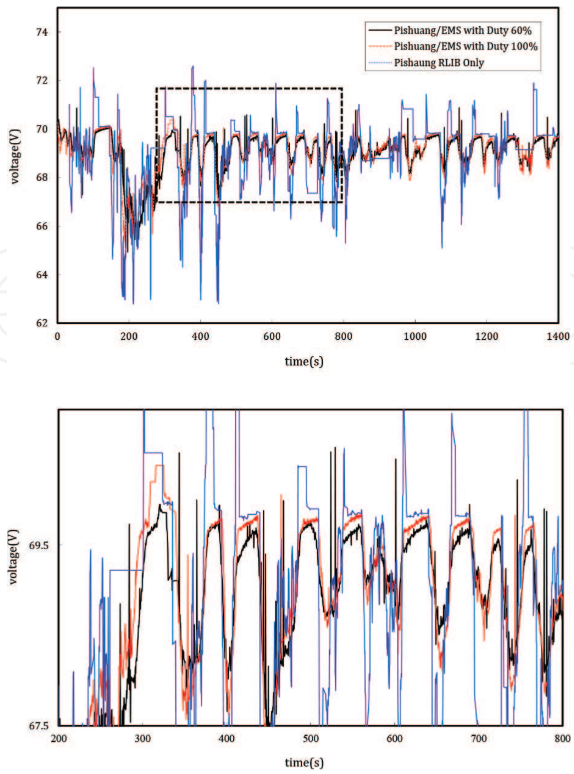

Figure 19. Comparison of DoD in single $LiFePO_4$ RLIB pack and RLIB with different PWM duty (upper: original; down: enlargement of dotted line in upper).

an auxiliary physical battery, individual IR of experimental batteries is listed in **Table 3**. IR of $LiFePO_4$ RLIB at 65.75 mΩ is much higher than that at 9.81 mΩ of $LiMnNiCoO_2$ RLIB pack and 3 mΩ of auxiliary physical battery (UC) by excluding harness resistance and fixture resistance. The load current provided by the auxiliary physical battery depends on each IR in parallel connection relative to RLIB (i.e., the lower the IR of the auxiliary physical battery, the higher current it can share) [42]. Consequently, a simple circuit converterless EMS in this study shows potential in controlling power flow to avoid the intense loading of RLIB. In particular, EMS with auxiliary high-power battery can increase the life cycle of RLIB [42]. Mass production of EMS has its potential in large-scale application of WWTPs. As **Figure 8** shows, average DoD in lifespan is nonlinear, which indicates that LIB can earn useful energy if average DoD is limited [44–48]. The distribution of DoD is directly related to life cycle as the formulation [48]. We apply this formulation to roughly estimate the benefit of using RLIB with EMS in this study.

10. Conclusion

In this study of applying RLIB in WWTP, a rough estimation by calculating the range of DoD by using EMS obtains the elongated range of an RLIB's life cycle up to 45% from 1100 to 1600 cycles at effective capacity of 80% based on the formulation in [48]. Under the consideration of environment, cost, and performance, the possibility of using automotive RLIBs is studied. One simple and converterless EMS is developed to use in a new RLIB pack. The bench test and rough estimation reveal that the EMS shows great potential in elongating life cycle and enhancing electricity charges. Furthermore, a simple, training-free, and easily implemented scheme based on ECM is applied in EMS. It is capable of online estimation of VOC and life cycle-sensitized IR for ensuring the safety of RLIB packs.

Next phase, a pilot run to install small-scale RLIB in Dihua plant is launched. For reflecting the best in-situ energy efficiency, remote power monitoring system is used to measure the peak and averaged energy consumption of aeration tank. It will function in the decision of optimized PWM signals for elongating the life cycle of RLIB.

Acknowledgements

This work was supported by government's budget, Water Resource Agency, Ministry of Economic Affairs in Taiwan under contract no. MOEAWRA1060474.

Author details

Yi-Hsien Chiang[1] and Wu-Yang Sean[2]*

*Address all correspondence to: wysean@cycu.org.tw

1 Gentec Inc., Taiwan

2 Department of Environmental Engineering, Chung Yuan Christian University, Chung-Li, Taiwan

References

[1] Argaw N. Renewable Energy in Water and Wastewater Treatment Applications. June 2003. NREL/SR-500-30383

[2] Olsson G. Water and Energy: Threats and Opportunities. London: IWA Publishing; 2012

[3] Mielke E, Anadon LD, Narayanamurti V. Water consumption of energy resource extraction, processing, and conversion. Harvard Kennedy School, Belfer Center for Science and International Affairs, Cambridge, MA, USA; Technical Report; October, 2010

[4] Energy Demands on Water Resources: Report to Congress on the Interdependency of Energy and Water. US Department of Energy; Technical Report; 2006

[5] Stillwell S, King CW, Webber ME, Duncan IJ, Hardberger A. The energy-water Nexus in Texas. Ecology and Society. 2011;**16**(1):2

[6] Park L, Croyle K. California water-energy nexus: Pathways to implementation. GEI Consultants Inc.; Technical Report; 2012

[7] Kokabian B, Gude VG. Photosynthetic microbial desalination cells (PMDCs) for energy, water and biomass production. Environmental Science: Processes & Impacts. 2013;**15**(12): 2178-2185

[8] Energy Production and Efficiency Research – The Roadmap to Net-Zero Energy. Water Environment Research Foundation. Fact Sheet. August 2011

[9] Evaluation of Energy Conservation Measures for Wastewater Treatment Facilities. United States: Environmental Protection Agency; 2010. pp. 4-5

[10] Gude VG, Nirmalakhandan N, Deng S. Desalination using solar energy: Towards sustainability. Energy. 2011;**36**(1):78-85

[11] Shoener BD, Bradley IM, Cusick RD, Guest JS. Energy positive domestic waste water treatment: The roles of anaerobic and photorophic technologies. Environmental Science: Processes & Impacts. 2014;**16**:1204-1222

[12] Wett B, Buchauer K, Fimml C. Energy self-sufficiency as a feasible concept for wastewater treatment systems. In: Proceedings of the IWA Leading Edge Technology Conference, Asian Water; 21-24 September, 2007; Singapore

[13] Arnold ME, Merta ES. Towards energy self-sufficiency in wastewater treatment by optimized sludge treatment. Water Practice and Technology. 2011;**6**(4). Article No: 7

[14] Mo W, Zhang Q. Can municipal wastewater treatment systems be carbon neutral? Journal of Environmental Management. 2012;**112**:360-367

[15] Gikas P. Wastewater treatment plants as net energy production factories. In: International Conference on Environmental and Hazardous Substance Management towards a Green Economy; 21-23 May, 2013; Bangkok, Thailand

[16] Bieker S, Cornel P, Wagner M. Semicentralised supply and treatment systems: Integrated infrastructure solutions for fast growing urban areas. Water Science and Technology. 2010;**61**:2905-2913

[17] Lemos D, Dias AC, Gabarrell X, Arroja L. Environmental assessment of an urban water system. Journal of Cleaner Production. 2013;**54**:157e165

[18] Funamizu N, Iida M, Sakakura Y, Takakuwa T. Reuse of heat energy in wastewater: Implementation examples in Japan. Water Science and Technology. 2001;**43**(10):277e285

[19] Nowak O, Keil S, Fimml C. Examples of energy self-sufficient municipal nutrient removal plants. Water Science and Technology. 2011;**64**(1):1-6

[20] Frijns J, Hofman J, Nederlof M. The potential of (waste) water as energy carrier. Energy Conversion and Management. 2013;**6**:357-363

[21] Meggers F, Leibundgut H. The potential of wastewater heat and exergy: Decentralized high-temperature recovery with a heat pump. Energy and Buildings. 2011;**43**:879-886

[22] Baber C. Tapping into waste heat. Journal of Water and Environment Technology. 2010; **22**:40-45

[23] Chae K-J, Kang J. Estimating the energy independence of a municipal wastewater treatment plant incorporating green energy resources. Energy Conversion and Management. 2013;**75**:664-672

[24] Wanner O, Panagiotidis V, Clavadetscher P, Siegrist H. Effect of heat recovery from raw wastewater on nitrification and nitrogen removal in activated sludge plants. Water Research. 2005;**39**:4725-4734

[25] Dürrenmatt D, Wanner O. A mathematical model to predict the effect of heat recovery on the wastewater temperature in sewers. Water Research. 2014;**48**:548-558

[26] Kretschmer F, Neugebauer G, Kollmann R, Eder M, Zach F, Zottl A, Narodoslawsky M, Stoeglehner G, Ertl T. Resource recovery from wastewater in Austria—Wastewater treatment plants as regional energy cells. In: Proceedings of the IWA World Water Congress and Exhibition; Lisbon, Portugal; 21-26 September 2014

[27] Woodbank Communications Ltd. Battery Performance Characteristics. Available from: http://www.mpoweruk.com/performance.htm

[28] Zhang T, He Y, Wang F, Ge L, Zhu X, Li H. Chemical and process mineralogical characterizations of spent lithium-ion batteries. Approach by multi-analytical techniques. Waste Management. 2014;**34**:1051-1158

[29] Zhang P, Yokoyama T, Itabashi O, Suzuki TM, Inoue K. Hydrometallurgical process for recovery of metal values from spent lithium-ion secondary batteries. Hydrometallurgy. 1998;**47**:259-271

[30] Manthiram A. Materials challenges and opportunities of lithium-ion batteries. The Journal of Physical Chemistry Letters. 2011;**2**:176-184

[31] Scrosati B, Garche J. Lithium batteries: Status, prospects and future. Journal of Power Sources. 2010;**195**:2419-2430

[32] Nitta N, Wu F, Lee JT, Yushin G. Li-ion battery materials: Present and future. Materials Today. 2015;**18**(5):252-264

[33] Pay S, Baghzouz Y. Effectiveness of battery-super capacitor combination in electric vehicles. In: IEEE Bologna PowerTech Conference; June 2003; pp. 728-733

[34] Cao J, Emadi A. A new battery/ultracapacitor hybrid energy storage system for electric, hybrid, and plug-in hybrid electric vehicles. IEEE Transactions on Power Electronics. 2012;**27**(1):122-132

[35] Nobuyuki Kasuga, Nobuhito Ohnuma. Ultra-Capacitor and Battery Hybrid EV with High Efficiency Battery Load Leveling System. EVS15(CD-ROM). 1995

[36] Grbovic PJ, Delarue P, Le Moigne P, Bartholomeus P. A bidirectional three-level DC–DC converter for the ultracapacitor applications. In: IEEE Transactions on Industrial Electronics; Vol. 57. Issue 10. Oct 2010; pp. 3415-3430

[37] Di Napoli, Crescimbini F, Solero L, Caricchi F, Capponi FG. Multiple-input DC-DC power converter for power-flow management in hybrid vehicles. In: IEEE International Conference on Industrial Applications: The 37th Annual Meeting, Vol. 3. 2002. pp. 1578-1585

[38] Kawashima K, Uchida T, Hori Y. Development of a novel ultracapacitor electric vehicle and methods to cope with voltage variation. In: IEEE Vehicle Power and Propulsion Conference; September, 2009

[39] Lu S, Corzine KA, Ferdowsi M. A new battery/ultracapacitor energy storage system design and its motor drive integration for hybrid electric vehicles. IEEE Transactions on Vehicular Technology. 2007;**56**(4):1516-1523

[40] Ortúzar M, Moreno J, Dixon J. Ultracapacitor-based auxiliary energy system for an electric vehicle: Implementation and evaluation. IEEE Transactions on Industrial Electronics. 2007;**54**(4):2147-2156

[41] Wu C-H, Hung Y-H, Sean W-Y. Development of a real-time simulator for electric vehicle with dual energy storage system, Li-ion battery and ultracapacitor. In: Workshop on Power Electronics and Intelligent Transportation System, PEITS; 2009

[42] Wu C-H, Chiang Y-H, Sean W-Y, Lo S-M, Ke J-C, Hung Y-H. Optimal designs and experimental verification for a hybrid energy storage system. In: IEEE Program Committee of 3CA; May 2010

[43] Sean W-Y, Chiang Y-H, Wu C-H, Liang Y-C, Ke J-C, Lo S-M. Feasibility of hybrid energy storage system for light electric vehicle. In: EVS-25 The 25th International Battery, Hybrid and Fuel Cell Electric Vehicle Symposium & Exposition; Shenzhen, China; November 5-9, 2010

[44] Peterson SB, Apta J, Whitacre JF. Lithium-ion battery cell degradation resulting from realistic vehicle and vehicle- to grid utilization. Journal of Power Sources. 2010;**195**:2385-2392

[45] Liaw BY, Jungst RG, Nagasubramanian G, Case HL, Doughty DH. Modeling capacity fade in lithium ion cells. Journal of Power Sources. 2005;**140**:157-161

[46] Ning G, Popov BN. Cycle life modeling of lithium ion batteries. Journal of the Electrochemical Society. 2004;**151**(10):A1584-A1591

[47] Ning G, White RE, Popov BN. A generalized cycle life model of rechargeable Li-ion batteries. Electrochimica Acta. 2006;**51**(10):2012-2022

[48] Wang J, Liu P, Hicks-Garner J, Sherman E, Soukiazian S, Verbrugge M, Tataria H, Musser J, Finamore P. Cycle-life model for graphite-$LiFePO_4$ cells. Journal of Power Sources. 2011;**196**:3942-3948

[49] https://ironedison.com/48-volt-lithium-battery-for-solar

[50] Hadjipaschalis I, Poullikkas A, Efthimiou V. Overview of current and future energy storage technologies for electric power applications. Renewable and Sustainable Energy Reviews. 2009;**13**:1513-1522

[51] Mwasilu F, Justo JJ, Kim E-K, Do T-D, Jin-WooJung. Electric vehicles and smart grid interaction: A review on vehicle to grid and renewable energy sources integration. Renewable and Sustainable Energy Reviews. 2014;**34**:501-516

[52] Renn G-z, Ma G-q, Cong N. Review of electrical energy storage system for vehicular applications. Renewable and Sustainable Energy Reviews. 2015;**41**:225-236

[53] Chiang Y-H, Sean W-Y, Ke J-C. Online estimation of internal resistance and open-circuit voltage of lithium-ion batteries in electric vehicles. Journal of Power Sources. 2011;**196**:3921-3932

IntechOpen